JOURNAL OF Materials CHEMISTRY

Fluorinated aminoalkoxide Cu^{II} complexes: new CVD precursors for deposition of copper metal

Yun Chi,*[a] Peng-Fu Hsu,[a] Chao-Shiuan Liu,*[a] Wei-Li Ching,[a] Tsung-Yi Chou,[a] Arthur J. Carty,*[b] Shie-Ming Peng,[c] Gene-Hsiang Lee[c] and Shiow-Huey Chuang[d]

[a]*Department of Chemistry, National Tsing Hua University, Hsinchu 30013, Taiwan. E-mail: ychi@mx.nthu.edu.tw*
[b]*Steacie Institute for Molecular Sciences, National Research Council Canada, 100 Sussex Drive, Ottawa, Ontario, Canada K1A 0R6*
[c]*Department of Chemistry and Instrumentation Center, National Taiwan University, Taipei 10764, Taiwan*
[d]*National Nano Device Laboratories, Hsinchu 30050, Taiwan*

Received 5th June 2002, Accepted 27th August 2002
First published as an Advance Article on the web 27th September 2002

Volatile low-melting Cu^{II} metal complexes of formula $Cu[OC(CF_3)R^1CH_2NHR^2]_2$ (R^1 = CF_3 or CH_3; R^2 = CH_2CH_2OMe, Bu^i, or Bu^t) and $Cu[OC(CF_3)R^1CH_2NMe_2]_2$ (R^1 = CF_3 or CH_3) have been synthesized and characterized by spectroscopic methods. A single-crystal X-ray diffraction study on $Cu[OC(CF_3)_2CH_2NHCH_2CH_2OMe]_2$ shows that one methoxyethyl group of the aminoalkoxide ligand forms an intramolecular dative bond to the Cu atom to produce a square-pyramidal geometry at the metal center, while the second is linked to the Cu atom of the adjacent molecule, giving an N_2O_4 octahedral coordination arrangement. For the second Bu^i-substituted complex, $Cu[OC(CF_3)_2CH_2NHBu^i]_2$, the X-ray structural analysis demonstrated an N_2O_2 square-planar geometry, with one alkoxide oxygen atom forming strong H-bonding to an adjacent water molecule. Metal CVD experiments were carried out, showing that the source reagents $Cu[OC(CF_3)_2CH_2NHBu^i]_2$, $Cu[OC(CF_3)_2CH_2NHBu^t]_2$, and $Cu[OCMe(CF_3)CH_2NHBu^i]_2$, which possess a secondary amino group, are capable of depositing copper metal at temperatures of 250–300 °C under inert Ar carrier gas, while $Cu[OCMe(CF_3)CH_2NMe_2]_2$, with a tertiary amine group, requires the use of reductive H_2 carrier gas to induce metal deposition at lower temperatures.

Copper metal thin films have great potential for fabricating metal interconnections as well as for filling contacts and vial holes designed for next-generation ultra large scale integrated (ULSI) circuit technology.[1] The advantages of copper over other conducting metals, such as aluminum, include lower resistivity, enhanced electromigration resistance, and increased resistance to stress-induced formation of voids due to a higher melting point. In addition, copper metal also provides improvements related to device performances, such as greater operation speed, reduced cross-talk and RC delay, *etc.*

The copper(II) hexafluoroacetylacetonate complex $Cu(hfac)_2$ has been used as a CVD source reagent to deposit copper metal.[2] Precursors of this type also include the related β-acetoacetate and β-ketoiminate Cu^{II} complexes.[3] The strategy of changing the coordination ligand is aimed at trying to increase the volatility and thermal stability of the complex, while also being able to induce the selective deposition of copper metal on patterned substrate surfaces and to lower the deposition temperature. For the parent complex $Cu(hfac)_2$, it was reported that pure copper thin film can be obtained in the presence of H_2 as a reducing agent.[4]

$$Cu(hfac)_2 + H_2 \rightarrow Cu_{(s)} + 2\ (hfac)H$$

Upon removal of the external reducing reagent, Cu^{II} diketonate source reagents leave an excess of carbon and other contaminants on the thin film due to unwanted heat-induced ligand fragmentation.[5] In addition, lower temperatures must be used in order to ensure clean conversion to the metallic state.

On the other hand, a second type of Cu^{I} CVD source reagent has been developed, for which the best known reagent is the complex (hfac)Cu(tmvs) (tmvs = trimethylvinylsilane), which has been used as an industry standard to deposit copper by the CVD method. Other established Cu^{I} CVD source reagents include (hfac)CuL, where L = phosphine ligands such as PMe_3 and PEt_3,[6] alkyne ligands such as 2-butyne, and olefins such as butadiene, 1,5-cyclooctadiene,[7] and 2-methyl-1-hexene-3-yne.[8] Using the parent complex (hfac)Cu(tmvs) as an example,[9] the deposition of copper is represented by the thermally-induced disproportionation reaction:

$$2\ (hfac)Cu(tmvs) \rightarrow Cu + 2\ tmvs + Cu(hfac)_2$$

However, the complex (hfac)Cu(tmvs) is thermally unstable and begins to decompose at temperatures above 55–60 °C. Thus, this metal complex must be stored in a refrigerator and the addition of a chemical stabilizer, such as free tmvs ligand, is needed to improve the stability.[10] Moreover, the conversion from the liquid to the vapor phase requires excessive heating, thus, the aging and decomposition of (hfac)Cu(tmvs) at higher temperatures causes many difficulties, such as extensive maintenance of the CVD apparatus due to premature precursor decomposition. In order to prevent decomposition, lower temperatures have to be used for vapor transport. As a result, this reduces the precursor vapor pressure, giving a low deposition rate, and eventually leads to the formation of rough metal surfaces and large variations in surface resistivity.

Accordingly, there is a demand for new CVD source reagents, which should possess the combined advantages of both Cu^{II} and Cu^{I} compounds mentioned above, namely higher thermal and oxidative stability in air during storage, higher vapor pressure under the designated CVD conditions,

and the capacity to induce copper deposition in the absence of a reducing carrier gas such as H_2.[11] In this paper, we will report our achievement in synthesizing copper source reagents that fulfill these essential requirements. Part of this investigation has already been published as a Communication.[12]

Experimental

General information and materials

Mass spectra were obtained on a JEOL SX-102A instrument operating in electron impact (EI) mode. The thermogravimetric analyses (TGA) were recorded on a Seiko TG/DTA 300 instrument under an atmospheric pressure of N_2 with a flow rate of 100 cm^3 min^{-1} and with a heating rate of 10 °C min^{-1}. Elemental analyses were carried out at the NSC Regional Instrumentation Center at National Cheng Kung University, Tainan, Taiwan. All aminoalkoxide ligands, $HOC(CF_3)_2CH_2NHR$, R = CH_2CH_2OMe, Bu^i and Bu^t, $HOC(CF_3)_2CH_2NMe_2$, $HOCMe(CF_3)CH_2NHBu^i$, and $HOCMe(CF_3)CH_2NMe_2$, were prepared according to the method reported in the literature.[13] All reactions were performed under N_2 using anhydrous solvents or solvents treated with an appropriate drying reagent.

The Cu metal thin films were studied using an X-ray diffractometer (XRD) with Cu-K_α radiation. Scanning electron microscopy (SEM) images were recorded on a Hitachi S-4000 system to study the surface morphology. The resistivities were measured using the four-point probe method at room temperature, for which the instrument was assembled using a Keithley 2182 nanovoltmeter and a Keithley 2400 constant current source. The composition of the thin film was determined by X-ray photoelectron spectroscopy (XPS) utilizing a Physical Electronics PHI 1600 system with an Al/Mg dual anode X-ray source. The surface composition in atom percent was measured from XPS spectra collected after 1–2 min sputtering with argon at 4 keV until a constant composition was obtained.

Synthesis of complex 1. Sodium hydride (0.15 g, 6 mmol) was suspended in 25 mL of THF. To this was added dropwise 1.26 g of aminoalcohol $HOC(CF_3)_2CH_2NHCH_2CH_2OMe$ (5 mmol) in THF (25 mL). The mixture was further stirred for 2 h until evolution of gas had ceased. The solution was filtered to remove the unreacted NaH. The filtrate was then transferred into a 100 mL reaction flask containing a suspension of $CuCl_2$ (0.40 g, 3.0 mmol) in THF (25 mL). This mixture was first stirred at room temperature for 4 h, giving a purple homogeneous solution along with an off-white NaCl precipitate. The precipitate was then removed by filtration, the filtrate was concentrated to dryness, and the resulting residue was purified by vacuum sublimation (193 mTorr, 72 °C), giving 1.20 g of the purple copper complex $Cu[OC(CF_3)_2CH_2NHCH_2CH_2OMe]_2$ (**1**, 2.1 mmol, 84%). Single crystals suitable for an X-ray diffraction study were grown from a mixture of CH_2Cl_2 and hexane at room temperature.

Spectral data for **1**: MS (EI, 70 eV, m/e^+, L = $C_7H_{10}F_6NO_2$), observed (actual) [assignment] {relative intensity}: 571 (571) [CuL_2] {3.14}, 502 (502) [$CuL_2 - CF_3$] {1.86}, 405 (405) [$CuL_2 - C_3F_6O$] {17.50}, 318 (317) [CuL] {100.00}, 254 (254) [L] {10.86}, 150 (151) [CuL − C_3F_6O] {59.69}, 88 (88) [L − C_3F_6O] {20.63}. Anal. calcd for $C_{14}H_{20}CuF_{12}N_2O_4$: C, 29.40; H, 3.53; N, 4.90; found: C, 29.48; H, 3.53; N, 4.92%.

Synthesis of complex 2. Procedures identical to those employed to prepare **1** were followed, using 0.15 g of sodium hydride (6 mmol), 1.26 g of the aminoalcohol ligand $HOC(CF_3)_2CH_2NHBu^i$ (5 mmol) and 0.37 g of $CuCl_2$ (2.8 mmol). After removal of THF solvent, vacuum sublimation (202 mTorr, 68 °C) gave the purple solid $Cu[OC(CF_3)_2CH_2NHBu^i]_2$ (**2**, 1.12 g, 2.0 mmol) in 79% yield. Single crystals suitable for an X-ray diffraction study were grown from a mixture of CH_2Cl_2 and hexane at room temperature.

Spectral data for **2**: MS (EI, 70 eV, m/e^+, L = $C_8H_{12}F_6NO$), observed (actual) [assignment] {relative intensity}: 567 (567) [CuL_2] {14.69}, 401 (401) [$CuL_2 - C_3F_6O$] {43.83}, 316 (315) [CuL_2 − L] {48.70}, 252 (252) [L] {29.22}, 148 (149) [CuL − C_3F_6O] {50.32}, 86 (86) [L − C_3F_6O] {100.00}, 69 (69) [CF_3] {9.90}, 57 (57) [C_4H_9] {12.66}. Anal. calcd for $C_{16}H_{24}F_{12}N_2O_2Cu$: C, 33.84; H, 4.26; N, 4.93; found: C, 32.92; H, 4.37; N, 4.96%.

Synthesis of complex 3. Procedures identical to those employed to prepare **1** were followed, using 0.15 g of sodium hydride (6 mmol), 1.26 g of the aminoalcohol ligand $HOC(CF_3)_2CH_2NHBu^t$ (5 mmol) and 0.37 g of $CuCl_2$ (2.8 mmol). After removal of THF solvent, vacuum sublimation (184 mTorr, 60 °C) gave the purple solid $Cu[OC(CF_3)_2CH_2NHBu^t]_2$ (**3**, 1.25 g, 2.2 mmol) in 88% yield.

Spectral data for **3**: MS (EI, 70 eV, m/e^+, L = $C_8H_{12}F_6NO$), observed (actual) [assignment] {relative intensity}: 567 (567) [CuL_2] {0.67}, 498 (498) [$CuL_2 - CF_3$] {1.31}, 401 (401) [$CuL_2 - C_3F_6O$] {47.18}, 385 (386) [$CuL_2 - C_3F_6O$-CH_3] {13.59}, 316 (315) [CuL] {50.77}, 300 (300) [CuL − CH_3] {18.08}, 260 (258) [CuL − C_4H_9] {11.79}, 238 (238) [L − CH_3] {100.00}, 148 (149) [CuL − C_3F_6O] {76.41}, 86 (86) [L − C_3F_6O] {96.41}, 69 (69) [CF_3] {9.90}, 57 (57) [C_4H_9] {12.66}. Anal. calcd for $C_{16}H_{24}CuF_{12}N_2O_2$: C, 33.84; H, 4.26; N, 4.93; found: C, 34.07; H, 4.32; N, 4.65%.

Synthesis of complex 4. Procedures identical to those employed to prepare **1** were followed, using 0.15 g of sodium hydride (6 mmol), 1.12 g of the aminoalcohol ligand $HOC(CF_3)_2CH_2NMe_2$ (5 mmol) and 0.37 g of $CuCl_2$ (2.8 mmol). After removal of THF solvent, vacuum sublimation (228 mTorr, 65 °C) gave the purple solid $Cu[OC(CF_3)_2CH_2NMe_2]_2$ (**4**, 0.92 g, 1.8 mmol) in 72% yield.

Spectral data for **4**: MS (EI, 70 eV, m/e^+, L = $C_6H_8F_6NO$), observed (actual) [assignment] {relative intensity}: 511 (511) [CuL_2] {0.33}, 442 (442) [$CuL_2 - CF_3$] {0.27}, 345 (345) [$CuL_2 - C_3F_6O$] {0.20}, 288 (287) [CuL] {0.25}, 224 (224) [L] {1.87}, 154 (154) [L − CF_3] {3.27}, 58 (58) [L − C_3F_6O] {100.00}. Anal. calcd for $C_{12}H_{16}CuF_{12}N_2O_2$: C, 28.16; H, 3.15; N, 5.47; found: C, 28.07; H, 3.50; N, 5.20%.

Synthesis of complex 5. Procedures identical to those employed to prepare **1** were followed, using 0.15 g of sodium hydride (6 mmol), 1.0 g of the aminoalcohol ligand $HOCMe(CF_3)CH_2NHBu^i$ (5 mmol) and 0.37 g of $CuCl_2$ (2.8 mmol). After removal of THF solvent, vacuum sublimation (350 mTorr, 90 °C) gave the purple solid $Cu[OCMe(CF_3)CH_2NHBu^i]_2$ (**5**, 0.73 g, 1.6 mmol) in 64% yield.

Spectral data for **5**: MS (EI, 70 eV, m/e^+, L = $C_8H_{15}F_3NO$), observed (actual) [assignment] {relative intensity}: 459 (459) [CuL_2] {7.81}, 347 (347) [$CuL_2 - C_3H_3F_3O$] {6.50}, 262 (261) [CuL] {90.79}, 198 (198) [L] {100.00}, 148 (149) [CuL − $C_3H_3F_3O$] {40.79}, 128 (129) [L − CF_3] {15.71}, 106 (106) [CuL − CF_3-CH_2N^iBu] {17.27}, 86 (86) [L − $C_3H_3F_3O$] {98.68}, 57 (57) [C_4H_9] {41.12}. Anal. calcd for $C_{16}H_{30}CuF_6N_2O_2$: C, 41.78; H, 6.57; N, 6.09; found: C, 41.78; H, 6.70; N, 6.24%.

Synthesis of complex 6. Procedures identical to those employed to prepare **1** were followed, using 0.15 g of sodium hydride (6 mmol), 0.85 g of the aminoalcohol ligand $HOCMe(CF_3)CH_2NMe_2$ (5 mmol) and 0.37 g of $CuCl_2$ (2.8 mmol). After removal of THF solvent, vacuum sublimation (350 mTorr, 90 °C) gave the purple solid $Cu[OCMe(CF_3)CH_2NMe_2]_2$ (**6**, 0.75 g, 1.85 mmol) in 74% yield.

Spectral data for **6**: MS (EI, 70 eV, m/e^+, L = $C_6H_{11}F_3NO$), observed (actual) [assignment] {relative intensity}: 403 (403) [CuL_2] {0.46}, 334 (334) [$CuL_2 - CF_3$] {0.10}, 291 (291) [$CuL_2 - C_3H_3F_3O$] {6.44}, 164 (164) [$CuL - CF_3$] {2.91}, 120 (121) [$CuL - C_3H_3F_3O$] {5.82}, 58 (58) [$L - C_3H_3F_3O$] {100.00}. Anal. calcd for $C_{12}H_{22}CuF_6N_2O_2$: C, 35.69; H, 5.49; N, 6.94; found: C, 35.83; H, 5.39; N, 7.12%.

X-Ray crystallography

Single-crystal X-ray diffraction data were measured on a Bruker SMART CCD diffractometer using Mo-K_α radiation (λ = 0.71073 Å). The data collection was executed using the SMART program. Cell refinement and data reduction were performed using the SAINT[14] program. The structure was solved using the SHELXTL/PC[15] program and refined using full-matrix least squares procedures. All non-hydrogen atoms were refined anisotropically, whereas hydrogen atoms were placed at the calculated positions and included at the final stage of refinements with fixed parameters. The crystallographic refinement parameters of complexes **1** and **2** are summarized in Table 1, and selected bond distances and angles are listed in Tables 2 and 3, respectively.

CCDC reference numbers 187010 and 187011.

See http://www.rsc.org/suppdata/jm/b2/b205419a/ for crystallographic data in CIF or other electronic format.

CVD procedures

Deposition of copper was carried out using a home-made vertical cold-wall reactor, consisting of a substrate holder placed at the center of a 20 × 20 × 20 cm^3 stainless steel CVD chamber (Fig. 1). The substrate holder was heated by a 600 W quartz lamp and controlled electronically. Working pressure during deposition was maintained at 0.2–0.35 Torr, with a typical background pressure of 1×10^{-3} Torr. Carrier gas was introduced through the sidearm of the sample reservoir, which was loaded with 50–75 mg of the source reagent during each CVD experiment. The flow rate of carrier gas was adjusted to 10–20 cm^3 min^{-1}. The deposition time was adjusted to 10–15 min. Before each experiment, the Si wafers were cleaned using a dilute HF solution, followed by washing with de-ionized water and acetone in sequence, and dried under nitrogen.

For experiments involving analysis of the organic co-products, the aminoalkoxide source reagent was passed through a long Pyrex tube of i.d. 25 mm under reduced pressure. The tubing was then placed within an electric temperature-controlled tube furnace, the heating block of which is about 30 cm long. The organic volatiles were then trapped at 77 K and dissolved into CD_2Cl_2 or acetone solution for both NMR analysis and GC-MS studies.

Table 1 X-Ray structural data for complexes **1** and **2**

Compound	**1**	**2**
Formula	$C_{14}H_{20}CuF_{12}N_2O_4$	$C_{16}H_{24}CuF_{12}N_2O_2{\cdot}H_2O$
Mol. wt.	571.86	585.93
Temperature	295 K	150 K
Crystal system	Triclinic	Triclinic
Space group	$P\bar{1}$	$P\bar{1}$
a/Å	11.0215(2)	9.9469(4)
b/Å	12.7768(2)	10.7389(4)
c/Å	13.2584(1)	12.8240(5)
α/°	98.494(1)	65.919(1)
β/°	102.203(1)	74.578(1)
γ/°	114.022(1)	83.479(1)
V/Å^3	1608.65(4)	1205.58(8)
Z	3	2
D_c/g cm^{-3}	1.771	1.614
F(000)	861	594
θ Range	1.63 to 26.37°	2.08 to 27.50°
h k l Ranges	−13–13, −15–15, −16–16	−12–12, −13–13, −16–16
Crystal size/mm.	0.36 × 0.12 × 0.12	0.45 × 0.16 × 0.10
μ(Mo-K_α)/mm^{-1}	1.145	1.018
Trans.: max, min.	0.831, 0.706	0.745, 0.862
Reflections collected	22 091	16 682
Independent reflections (R_{int})	6461 (0.0316)	5522 (0.0298)
Data/restraints/parameters	6461/0/449	5522/0/318
Goodness-of-fit on F^2	1.013	1.006
Final R indices [$I > 2\sigma(I)$]: R_1, wR_2	0.0435, 0.0932	0.0291, 0.0604
R indices (all data): R_1, wR_2	0.0614, 0.1011	0.0513, 0.0637
Extinction coefficient	0.0012(5)	
Largest diff. peak and hole/e Å^{-3}	0.393 and −0.379	0.324 and −0.352

Table 2 Selected bond distances (Å) and angles (°) for complex **1** (esds in parentheses)

Molecule 1			
Cu(1)–O(2)	1.926(3)	Cu(1)–O(4)	1.898(3)
Cu(1)–N(1)	1.999(3)	Cu(1)–N(2)	2.043(3)
Cu(1)···O(3)	2.629(3)	O(2)–C(5)	1.380(4)
C(4)–C(5)	1.556(4)	N(1)–C(4)	1.474(5)
O(4)–C(12)	1.365(5)	C(11)–C(12)	1.554(5)
N(2)–C(11)	1.486(5)		
∠O(2)–Cu(1)–O(4)	161.1(1)	∠N(1)–Cu(1)–N(2)	164.0(1)
Molecule 2			
Cu(2)–O(6)	1.897(3)	Cu(2)–N(3)	2.017(3)
Cu(2)···O(1)	3.873(3)	O(6)–C(19)	1.368(4)
C(18)–C(19)	1.550(4)	N(3)–C(18)	1.479(4)
∠O(6)–Cu(2)–N(3)	86.5(1)		

Table 3 Selected bond distances (Å) and angles (°) for complex **2** (esds in parentheses)

Molecule 1			
Cu(1)–O(1)	1.886(2)	Cu(1)–N(1)	2.017(2)
O(1)–C(6)	1.375(3)	C(5)–C(6)	1.546(3)
N(1)–C(5)	1.479(3)	O(1)···H(3B)	2.02(2)
∠O(1)–Cu(1)–O(1A)	180.0	∠N(1)–Cu(1)–N(1A)	180.0
∠O(1)–Cu(1)–N(1)	86.43(6)	∠O(1)–Cu(1)–N(1A)	93.57(6)
Molecule 2			
Cu(2)–O(2)	1.885(2)	Cu(2)–N(2)	2.028(2)
O(2)–C(14)	1.372(2)	C(13)–C(14)	1.547(3)
N(2)–C(13)	1.486(3)	O(2)···H(3C)	2.01(2)
∠O(2)–Cu(2)–O(2A)	180.0	∠N(2)–Cu(2)–N(2A)	180.0
∠O(2)–Cu(2)–N(2)	86.07(6)	∠O(2)–Cu(2)–N(2A)	93.93(6)

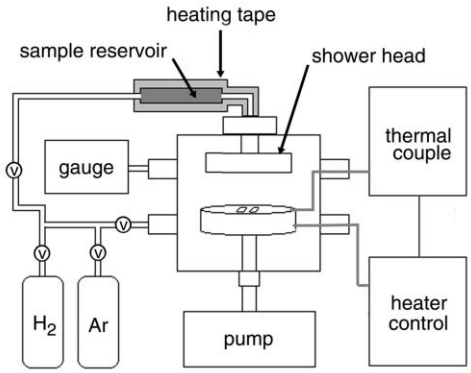

Fig. 1 Schematic diagram of the set-up of the cold-wall CVD apparatus.

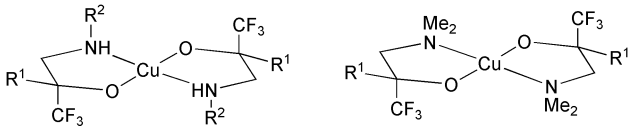

$R^1 = CF_3$, $R^2 = CH_2CH_2OMe$ (**1**)
$R^1 = CF_3$, $R^2 = Bu^i$ (**2**)
$R^1 = CF_3$, $R^2 = Bu^t$ (**3**)
$R^1 = Me$, $R^2 = Bu^i$ (**5**)

$R^1 = CF_3$ (**4**)
$R^1 = Me$ (**6**)

Scheme 1

Results and discussion

Synthesis and characterization

The copper CVD source reagents synthesized in this study consisted of a Cu^{II} metal center encapsulated by two chelating fluorinated β-aminoalcohol ligands. The latter were prepared in good yields by mixing an amine with a fluorinated oxirane, $(CF_3)_2\overline{COCH_2}$ or $(CF_3)Me\overline{COCH_2}$, in diethyl ether solution at room temperature, which was *in situ*-generated from hexafluoroacetone or trifluoroacetone and diazomethane etherate.[16] Subsequently, the copper complexes were prepared using a method related to that designed for the analogous metal complex $Cu[OC(CF_3)_2CH_2NH_2]_2$, involving prior treatment of the aminoalcohol ligand with excess NaH to generate the anionic ligand fragment, followed by addition of the aminoalcoholate into a THF suspension of $CuCl_2$. Finally, the products were purified by vacuum sublimation and recrystallization from a mixture of CH_2Cl_2 and hexane (Scheme 1). Notably, all these metal complexes are soluble in organic solvents such as CH_2Cl_2 or acetone, and their excellent stability in air is comparable to those of the fluoroalkoxide complexes $Cu(en)_2(OR_F)_2$ and $Cu(py)_2(OR_F)_2$, where OR_F = hexafluoro-*iso*-propoxo or hexafluoro-*tert*-butoxo groups.[17]

For structural identification, a single-crystal X-ray diffraction study on the complex $Cu[OC(CF_3)_2CH_2NHCH_2CH_2OMe]_2$ (**1**) has been carried out to confirm the exact structure in the solid state. As indicated in Fig. 2, two crystallographically and structurally different molecules are observed within the unit cell, with one metal complex located at a special position, the inversion center. The relevant bond lengths and angles are listed in Table 2. The average Cu–N distance is 2.020 Å, which is longer than the average value of the Cu–O distances (1.907 Å) and is comparable to that observed in the dimer complex $[Cu(hfac)(OCH_2CH_2NMe_2)]_2$ [2.020(5) Å].[18] However, the structures of these two molecules differ greatly from one another. This is evident from the fact that the methoxyethyl group of the first molecule resides on the same side of the N_2O_2 square-planar arrangement. The first methoxyethyl group forms an intramolecular dative bond to the central Cu atom, showing a short Cu(1)–O(3) intramolecular bond distance of 2.628 Å, which completes a distorted square-pyramidal coordination geometry for this molecule. Moreover, the second methoxyethyl group is found to coordinate to the Cu(2) atom of the adjacent molecule, which is indicated by a dashed line connecting these atoms in Fig. 2, with a longer Cu(2)–O(1) bonding interaction of 3.874 Å. As the Cu(2) atom of this molecule is located on the crystallographic center of inversion, it automatically generates a second, intermolecular O→Cu dative interaction located at the *trans*-position to the Cu(2)–O(1) bond. Consequently, the copper metal atom of the second complex is surrounded by a distorted octahedral arrangement involving two oxygen atoms derived from the methoxyethyl group, two alkoxide oxygen atoms, and two amino nitrogen atoms located at mutually *trans*-positions. This observed structure is very similar to that observed in the six-coordinate complex $Cu(hfac)_2(pyrazine)_2$, in which the two pyrazine donor ligands adopt a *trans*-geometry, while two hfac chelating ligands reside in the square plane.[19]

For the purposes of comparison, an X-ray diffraction study of a second Cu^{II} aminoalkoxide complex, $Cu[OC(CF_3)_2CH_2NHBu^i]_2$ (**2**), was also conducted to reveal the consequences of removal of the methoxyethyl substituent from the ligands. As shown in Fig. 3, this complex shows two essentially identical molecules in the asymmetric unit, each have their Cu atom located on an inversion center. Moreover, these two independent

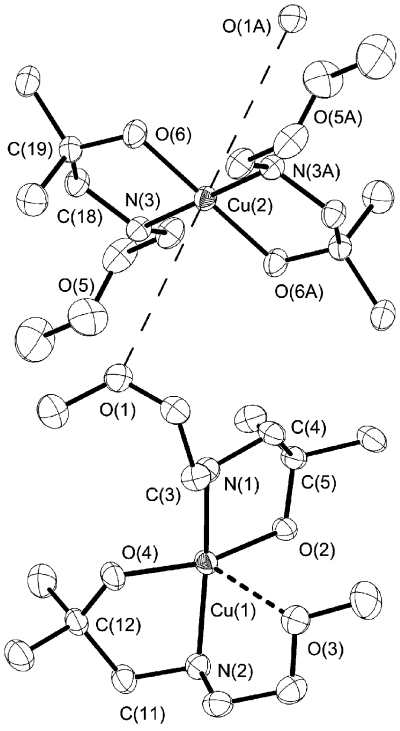

Fig. 2 ORTEP drawing of complex **1**, with thermal ellipsoids shown at 30% probability level. All the fluorine atoms of the CF_3 substituents have been removed for clarity.

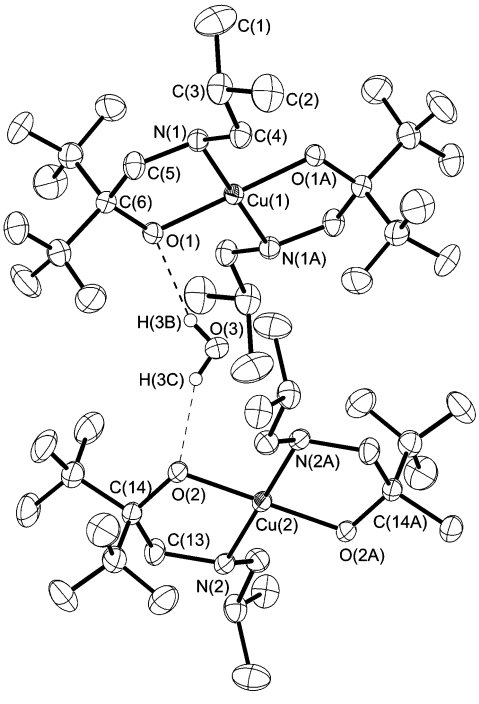

Fig. 3 ORTEP drawing of complex **2**, with thermal ellipsoids shown at 50% probability level.

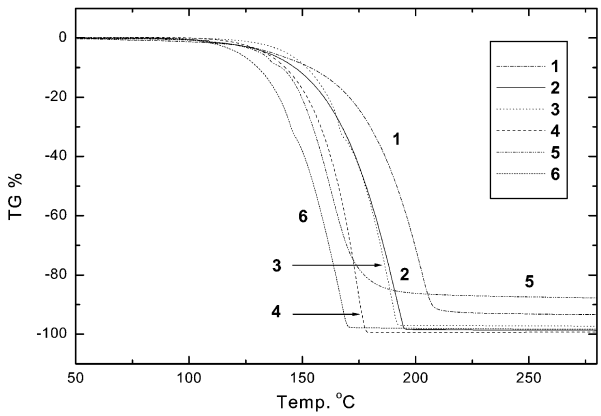

Fig. 4 Thermogravimetric analysis data; all experiments were carried out at atmospheric pressure with N_2 as carrier (100 cm^3 min^{-1}) and a heating rate of 10 °C min^{-1}.

molecules are linked to each other through a pair of intermolecular H-bonds to a water solvate [O(1)···H(3B) = 2.02(2) and O(2)···H(3C) = 2.01(2) Å], which is presumably incorporated into the crystal lattice during recrystallization. These results are in contrast to those reported for the related Cu^{II} metal complex $Cu(hfac)_2 \cdot H_2O$,[20] for which the strongly bonded water solvate is located at the axial site with a much shorter Cu–O(H_2O) distance of 2.204(3) Å. Moreover, the molecular structure of **2** adopts a *trans*-disposition for the N_2O_2 square framework, as well as for the *iso*-butyl substituent of the amino fragments. The average Cu–O distance of 1.886 Å and Cu–N distance of 2.023 Å are similar to those of the previously discussed methoxyethyl complex **1**. The chelating nature of the aminoalcoholate ligand leads to the formation of a five-membered ring structure, causing the corresponding O–Cu–N angle of ~86.2° to deviate slightly from the ideal value of 90° for a perfect square-planar arrangement.

After understanding their molecular structures, we then proceeded to investigate the physical data relevant to chemical vapor deposition. We observed that these copper complexes are fairly volatile and can be readily sublimed below 90 °C under a vacuum of 350 mTorr. Thermogravimetric analyses (TGA) were carried out at atmospheric pressure under N_2 and the data are plotted as the relative weight loss in wt% as a function of the temperature, for a heating rate of 10 °C min^{-1}. (Fig. 4). It is notable that the complex **1** shows the lowest volatility among these compounds. Its rapid loss of weight, which started at approximately 150 °C due to sample evaporation, is not complete until 210 °C, leaving approximately 4.0 wt% of solid residue at ~300 °C. We speculate that the reduced volatility is due to the coordination of the pendent methoxyethyl group to the nearby molecule, as observed in its solid-state structure. The derivative **5**, for which each of the aminoalkoxide chelate ligands contains only one CF_3 substituent, gave the highest residue weight, 12 wt%, upon raising the temperature. This residue exhibits a lustrous red color, somewhat similar to bulk copper. Moreover, as the observed residue weight is slightly lower than the weight percentage of copper in the sample (13.8%), this observation suggests that the majority of the sample may undergo thermal decomposition rather than vaporization during TG analysis, and it would probably give a better copper deposit at the lower temperatures employed for actual CVD experiments.

Complex **6** shows the highest volatility of all the samples examined, as the residual weight of this sample dropped to zero at only 170 °C, the lowest temperature recorded for any of the complexes. The enhanced volatility of **6** is attributed to a combination of (a) the lower molecular weight of **6** compared to the other complexes and (b) the replacement of the secondary amino group (CH_2NHR) found in **1**–**3** and **5** with a tertiary amino group (CH_2NMe_2). The second factor appears to be more important, as the presence of the secondary NHR group would typically give stronger intermolecular N–H···O hydrogen bonding between the alkoxide oxygen atom and hydrogen atom of this functional group. In agreement with this proposition, N–H···O hydrogen bonding has been observed as a key driving force for constraining an analogous aminoalkoxide fragment (L) into a fixed conformation, giving rise to a 10-membered metal wheel compound of formula $[Cu^{II}Cl(L)]_{10}$ [L = $OC(CF_3)_2CH_2NHCH_2CH_2NMe_2$].[21]

Other physical constants relevant to the CVD experiments are listed in Table 4. It appears that complex **1** shows the lowest melting point (87–88 °C) among all the copper complexes. Thus, it has the potential to serve as a liquid precursor, taking advantage of a stable rate of sample evaporation.[22] The decrease in melting point is apparently caused by the formation of inter- and intramolecular Cu–O coordination between Cu^{II} cations and methoxyl substituents. Moreover, complex **4**, with the tertiary CH_2NMe_2 group, is the derivative which decomposes at the highest temperature (232 °C). Therefore, this complex may require the highest temperature to induce spontaneous decomposition in the absence of reductive carrier gas.

Deposition of copper metal

Thermogravimetric analysis showed that all the Cu^{II} aminoalkoxide complexes prepared in this study can be volatilized below 150 °C under atmospheric pressure with almost no decomposition. Hence, these complexes should be potentially suitable for CVD use and, for complexes **2**, **3**, and **5**, deposition of copper metal has been achieved using an inert carrier gas (Ar) at temperatures of 250–325 °C in a standard cold-wall reactor. The run conditions selected for the CVD experiments and basic properties of the thin films are listed in Table 5. In general, growth of smooth copper metal thin films was realized under all conditions, and the as-deposited thin films were found to be reflective and have good adhesion.

The first Cu thin film was deposited using complex **2** as the source reagent and argon as the carrier gas (film 1). The SEM photo of this film [Fig. 5(1a)] shows formation of a dense microstructure with grain sizes in the range 100–300 nm. Preliminary XPS analysis revealed a composition of >98% copper metal, along with approximately 2% carbon, while other impurities, such as oxygen and fluorine, were not observed.

Table 4 Physical properties of the Cu^{II} source reagents

Compound	Formula	M. p./°C	Decomp. temp/°C	$T_{1/2}$[a]/°C	Residue[b]/wt%
1	$Cu[OC(CF_3)_2CH_2NHCH_2CH_2OMe]_2$	87–88	170	190	4.0
2	$Cu[OC(CF_3)_2CH_2NHBu^t]_2$	121–122	159	176	1.3
3	$Cu[OC(CF_3)_2CH_2NHBu^t]_2$	167–168	202	178	2.7
4	$Cu[OC(CF_3)_2CH_2NMe_2]_2$	177–178	232	166	0.8
5	$Cu[OCMe(CF_3)CH_2NHBu^t]_2$	130–131	160	162	12.0
6	$Cu[OCMe(CF_3)CH_2NMe_2]_2$	145–146	194	154	0.9

[a]The temperature at which 50 wt% of the sample has been lost during TGA analysis (N_2 flow rate = 100 cm^3 min^{-1}). [b]Total wt% of the sample observed at 500 °C during TGA analysis.

Table 5 Data obtained from CVD experiments using the Cu^{II} source reagents **2**, **3**, **5**, and **6**[a]

Film no. (source cpd)	Gas (flow rate/ cm^3 min^{-1})	T_S/°C	T_D/°C	P_S/ Torr	Film thickness/Å	Deposition rate/Å min^{-1}	Film resistivity, ρ/μΩ cm	Film contents
1 (**2**)	Ar (35)	150	250	0.2	800	133	4.9	Cu, >98%; C, <2%.
2 (**2**)	H_2 (25)	150	250	0.2	600	140	7.2	Cu, >98%; C, <2%.
3 (**2**)	H_2 (25)	150	275	0.2	1600	133	3.7	Cu, >99%; C, <1%.
4 (**2**)	H_2 (25)	150	300	0.2	2200	73	19.8	Cu, >98%; C, ~1%; O, F, <1%.
5 (**2**)	H_2 (25)	150	325	0.2	2300	140	22.2	Cu, >95%; C <4%; O, F, <1%.
6 (**3**)	Ar (10)	110	300	1	2400	60	16.4	Cu, >97%; C, O, F, <3%.
7 (**5**)	Ar (35)	130	250	0.2	2640	176	2.9	Cu, >99%; C, O, F, <1%.
8 (**6**)	Ar (15)	70	325	1	N. A.		N. A.	Cu, <53%; C, >27%
9 (**6**)	H_2 (15)	70	325	1	2500	167	5.7	Cu, >98%; C, <1%; O, F, <1%

[a] T_S: source temperature; T_D: deposition temperature; P_S: system pressure.

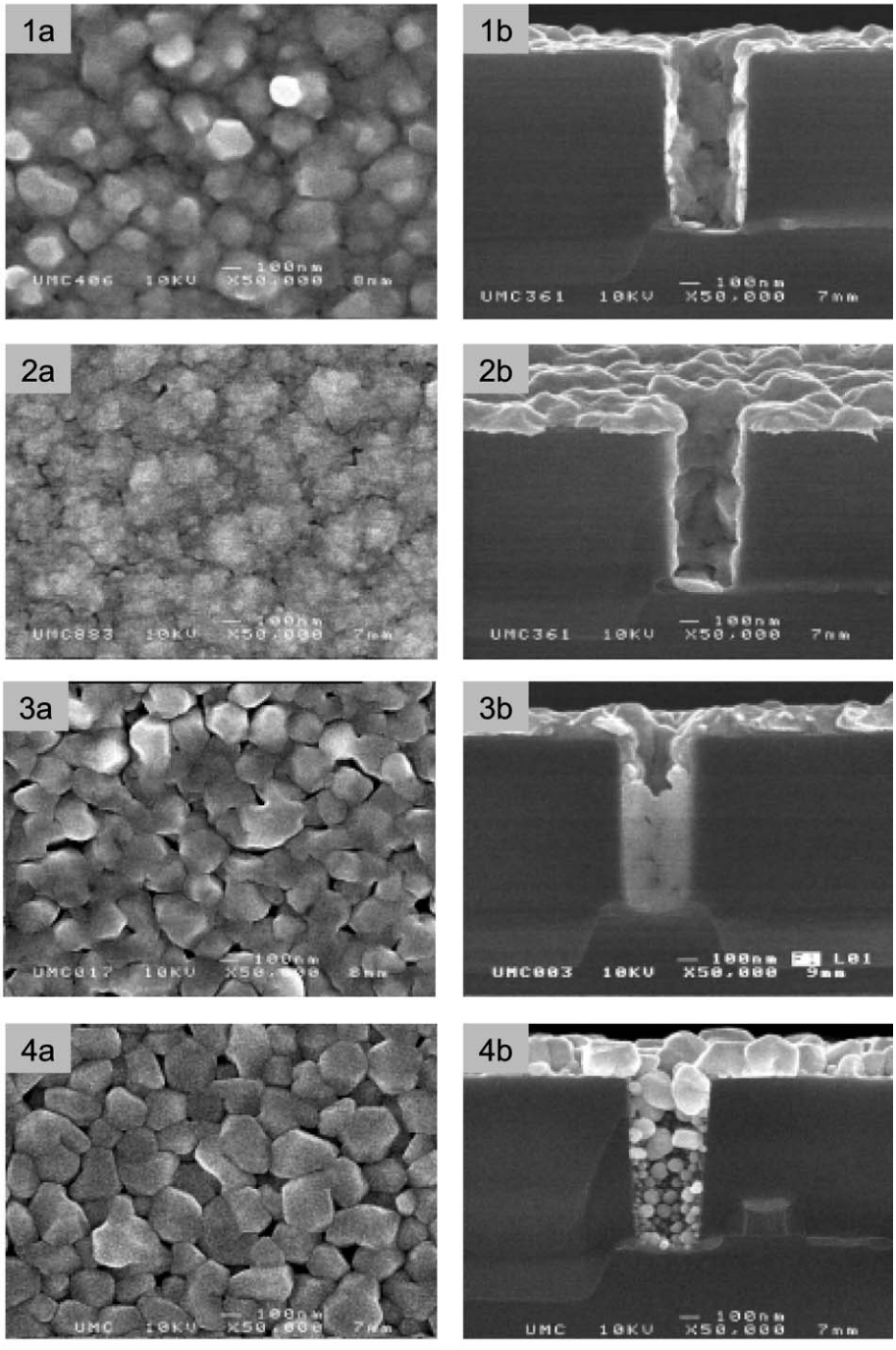

Fig. 5 SEM micrographs of the Cu films deposited using complex **2** as the source reagent: (1a and 1b) under Ar at 250 °C; (2a and 2b) under H_2 at 250 °C; (3a and 3b) under H_2 at 275 °C; (4a and 4b) under H_2 at 300 °C.

Four-point probe measurements gave a resistivity of 4.9 μΩ cm (800 Å), which is slightly higher than that of bulk copper (1.7 μΩ cm). The observed physical characteristics of the thin film suggest that the aminoalkoxide complex **2** should possess the capacity to deposit copper metal in the absence of an external reducing reagent, which is not the case for Cu^{II} source reagents such as $Cu(hfac)_2$ or even $Cu(acac)_2$.

The deposition reactions were next carried out using H_2 carrier gas to investigate the possible effect of an external reductant (film 2). A copper thin film with a slightly smoother morphology is obtained under these conditions [Fig. 5(2a)], for which the purity and the electrical resistivity show no further improvement compared with the sample prepared under Ar carrier gas. Upon increasing the temperature to 275 °C, the thickness of the thin film nearly doubled, showing a much faster rate of deposition, as expected for a temperature-dependent process [Fig. 5(3a)]. The thin film consists of well-defined microcrystalline grains, and several small voids are also visible at the grain boundaries. It appears that the physical characteristics of this thin film sample are optimal for the source reagent **2**; the resistivity is close to 3.7 μΩ cm and the metal purity is approaching 99%. On further increasing the deposition temperature to 300 °C, the thickness and the morphology of the thin film remain about the same [Fig. 5(4a)], but the resistivity and the purity dropped slightly with respect to the film obtained at 275 °C. This result is consistent with the occurrence of a slightly contaminated metal thin film at the higher temperature. We therefore assume that both Ar and H_2 can be used as the carrier gas and that the optimum temperature for copper deposition is about 275 °C, as used in this series of investigations. Moreover, the purity, as well as the resistivity, of the as-deposited copper thin films shows a continuous degradation upon further increasing the deposition temperature to 325 °C (see the analytical data for film 5 in Table 5).

In order to determine the conformal deposition on substrate surfaces, we chose a patterned wafer containing vial holes with a diameter of 0.4 μm and an aspect of ~2, and repeated thin film depositions under the conditions described for films 1–4. A thin layer of TiN was applied to these patterned wafers to serve as a diffusion barrier and to improve the copper metal adhesion. Fig. 5(1b) and (2b) show SEM pictures of the films resulting from deposition at the lowest temperature (250 °C) under Ar and H_2 carrier gas, respectively. It is clear that the vial hole has been covered with a thin layer of copper metal in both experiments. Although the surface of the resulting copper film is rather rough, we estimate that the thickness of the copper film within the vial hole is about two times thinner than that of the copper deposited on the more exposed top layer, an indication of lower step coverage.

Upon raising the temperature to 275 °C, the faster reaction on the substrate surface causes a substantial increase in copper deposition at all positions, giving a better conformal coverage, which is shown in Fig. 5(3b). We believe that this will provide the optimum conditions for completely filling the vial holes with copper metal if the deposition time is increased and a sufficient amount of CVD source reagent is provided. Finally, on further increasing the temperature to 300 °C, it can be seen that both the copper deposition and the grain growth reaction becomes much faster on the top surface [Fig. 5(4b)], and the formation of larger copper crystallites severely blocks the entrance to the vial hole and prevents the source reagent from diffusing into the bottom layer. Accordingly, a very small amount of copper is deposited into the vial hole, showing the deleterious effect of excessively high temperatures.

Fig. 6 shows the X-ray diffraction patterns (XRD) of the copper films deposited under Ar and H_2 at all three deposition temperatures (250, 275, and 300 °C). For the experiments that were conducted at 250 °C, the thin films look amorphous, exhibiting weak diffraction signals, which are also consistent with the SEM picture, which shows a smooth and featureless

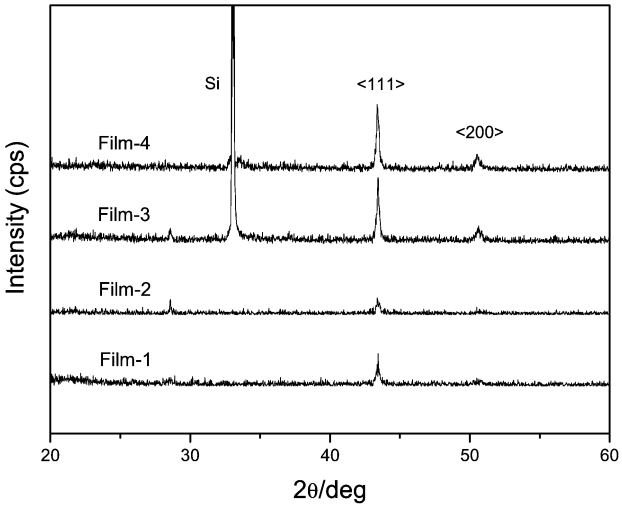

Fig. 6 X-Ray diffraction patterns of the as-deposited copper thin films: the labeling of each diffraction pattern is identical to those listed in Table 5.

surface morphology. However, the XRD diffraction signals at $2\theta = 43.6$ and 50.7° become more intense upon raising the temperature to 275 and then to 300 °C. The intensity of these diffraction peaks exhibits a constant intensity ratio of 4 : 1 at these temperatures, showing that the as-deposited thin films have an fcc structure with (111) preferred orientation. As this preferred orientation is known to prevent electromigration of the metal layer, the thin films obtained at temperatures between 275 and 300 °C should show good resistance to failure.[23]

The CVD experiments have also been executed using other source reagents, complexes **3**, **5**, and **6**, to determine the effect of the different substituents on the aminoalkoxide chelate ligands. The first experiment involved the use of the *t*-butyl derivative, complex **3**, conducted under Ar carrier gas at a temperature of 300 °C (film 6). Although the basic properties of the thin film look only slightly inferior to those of the previously discussed films prepared using source reagent **2**, the SEM photo shown in Fig. 7(a) shows the formation of large voids and cracks at the grain boundaries on the substrate surface. This change in surface morphology would appear to result from the different alkyl substituents of the ligand in **6**, but this cannot be stated with any certainty at present.

For deposition experiment using complex **5** as the source reagent, a light red and adherent thin film of thickness 2640 Å, containing over 99% Cu metal, was obtained under Ar at 250 °C (film 7). The electrical resistivity of this film ($\rho = 2.9$ μΩ cm) is very close to the physical limit of the resistivity of bulk copper (1.7 μΩ cm). In good agreement with these physical data, the SEM photo shows the formation of closely packed microcrystalline grains [Fig. 7(b)], suggesting that source reagent **5** has equally good potential for depositing Cu film as complex **2**.

We speculate that the excellent behavior of compound **5** is caused by replacement of one CF_3 group with a less electron-withdrawing methyl substituent, which reduces the thermal stability of the copper complex and, in turn, allows the deposition of metal to occur at a lower temperature, resulting in the inclusion of less impurities. This fine tuning of the structure means that complex **5** (with one CF_3 and one Me group at the alkoxide α-position) has a stability intermediate between those of complex **2** (with two CF_3 groups) and their non-fluorinated aminoalkoxide analogues, such as $Cu[OCH_2CH_2NMe_2]_2$ and $Cu[OCHMeCH_2NMe_2]_2$,[24] thus giving the observed CVD results.

Finally, the CVD experiments were performed using the source reagent **6**, which contains a tertiary amino functional group at the chelating alkoxide ligands. As indicated in

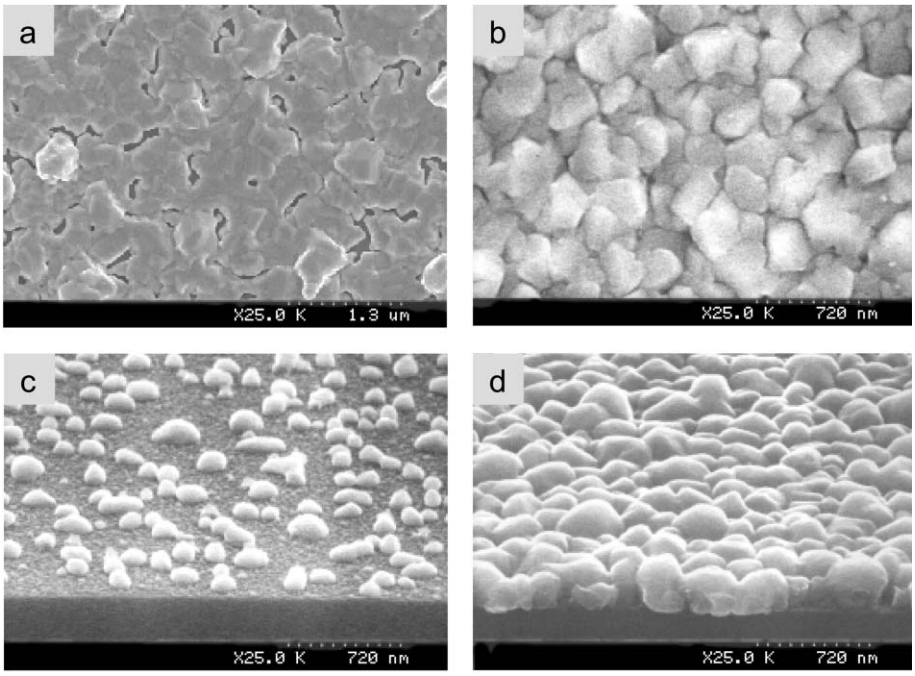

Fig. 7 SEM micrographs of the Cu films deposited using copper complexes **3**, **5**, and **6**: (a) using **3** as source reagent under Ar at 300 °C; (b) using **5** as source reagent under Ar at 250 °C; (c) using **6** as source reagent under Ar at 325 °C; (d) using **6** as source reagent under H_2 at 325 °C.

Fig. 7(c), there is no formation of a continuous thin film for a deposition experiment conducted under Ar carrier gas at a temperature of 325 °C (film 8). Under these conditions, only a few copper metal droplets spreading over the substrate surface are observed, which shows a typical situation for the nucleation and growth of copper nanoparticles during the initial stage of deposition.[25] This observation unambiguously confirms that the source reagent **6** is unsuitable for the deposition of thin films under these conditions, for which the selected deposition temperature is at least 50 °C higher than that utilized for the CVD experiments using source reagents **2**, **3**, and **5**. However, by changing the carrier gas from Ar to H_2, formation of good quality, copper thin film was clearly evidenced (film 9). The SEM photo of the resulting thin film is shown in Fig. 7(d), revealing a surface morphology consisting of granular, densely packed microcrystallites with diameters of ~300 nm. This suggests that a reducing agent such as H_2 is capable of inducing a clean conversion to copper metal.

Possible reaction mechanism

Delineation of the exact mechanism that afforded the pure copper metal is of interest, and we speculate that the chemistry should be somewhat related to that of the previously reported aminoalkoxide complexes $Cu[OCH_2CH_2NMe_2]_2$ and $Cu[OCHMeCH_2NMe_2]_2$,[26] for which the thermal deposition of copper metal occurred according to the proposed reaction given below.

$$Cu(OCHRCH_2NMe_2)_2 \rightarrow Cu_{(s)} + O{=}CRCH_2NMe_2 + HOCHRCH_2NMe_2 \ (R = H \text{ or } Me)$$

In this system, the conversion from Cu^{II} to Cu^0 is believed to proceed by formation of dimethylaminoethanal for R = H (or dimethylaminoacetone for R = Me) *via* β-hydrogen elimination, giving a transient copper hydride intermediate. Subsequent hydride transfer to the second dimethylaminoethoxide chelate would give rise to the formation of the free dimethylaminoethanol observed.

Accordingly, as we have incorporated two Me and CF_3 groups adjacent to the alcoholate group of our Cu^{II} complexes, direct conversion from alcoholate to an aldehyde or ketone group is not feasible in this case, simply because they have no accessible β-hydrogen atom within the coordinated ligand. On the other hand, as complexes **2**, **3**, and **5** possess secondary amino functional groups, this unique molecular architecture would allow formation of an imino fragment *via* a dehydrogenation reaction. The hydrogen atom(s) released would then transfer to the oxygen atom of the second alcoholate, leading to the formation of copper metal and an equal amount of iminoalcohol and aminoalcohol:

$$Cu[OC(CF_3)R^1CH_2NHR^2]_2 \rightarrow Cu_{(s)} + HOC(CF_3)R^1CH_2NHR^2 + HOC(CF_3)R^1CH{=}NR^2 \ (R^1 = CF_3 \text{ or Me; } R^2 = Bu^t \text{ or } Bu')$$

This postulated decomposition pathway is partially supported by a literature report involving facile oxidation of a secondary amine with a Cu^{II} oxidant in THF at room temperature, in which the Cu^{II} oxidant is generated *in situ* from mixing equal amounts of $CuBr_2$ and $LiOBu'$.[27]

Alternatively, we propose a second pathway that involves the formation of a fluorinated ketone molecule, $CF_3(R^1)C{=}O$ and an imine fragment, $H_2C{=}NR^2$, as well as the corresponding aminoalcohol, according to the transformation below.

$$Cu[OC(CF_3)R^1CH_2NHR^2]_2 \rightarrow Cu_{(s)} + CF_3(R^1)C{=}O + H_2C{=}NR^2 + HOC(CF_3)R^1CH_2NHR^2$$

The ketone and the imine could possibly be produced *via* a C(α)–C(β) bond fission reaction and a co-operative hydrogen transfer from the nitrogen atom of one aminoalcoholate to the oxygen atom of the second ligand while, concurrently, the central Cu^{II} ion is reduced to the Cu^0 state. According to the literature, the oxidation of a β-aminoalcohol in solution by electrochemical methods would afford the related imine intermediate and the ketone product by cleavage of the carbon–carbon bond between the hydroxyl and the amine functional groups.[28]

In order to shed light on the reaction mechanism of the metal deposition process, we collected the volatile organic co-products and analyzed the constituents. We decided to select the source reagent **3** as the target for this study, since the *t*-butyl substituent of the amino alkoxide ligand would simplify the NMR spectra and assist the interpretation of spectral data.

The organic volatiles were dissolved in d_6-acetone solution and this solution was then subjected to NMR analysis. The ^{1}H NMR spectrum shows seven signals at δ 4.68 (~4), 4.09 (100), 3.29 (~4), 3.02 (~4), 1.29 (~12), 1.11 (~15), and 1.10 (~15%), with approximate integration ratios for the peaks included in parentheses. The strongest signal at δ 4.09 is identified as due to the hydroxyl group of hexafluoroacetone hydrate, since the observed chemical shift is identical to that of a commercial sample and the water was probably inadvertently introduced during preparation of the NMR sample solution. The pair of signals at δ 3.02 and 1.10 correspond to the CH_2 and Bu^t groups of the dissociated aminoalcohol ligand $HOC(CF_3)_2CH_2NHBu^t$. Subtraction of these signals from the NMR spectrum leaves two CH_2 signals of equal intensity at δ 4.681 and 3.293, and one Bu^t signal at δ 1.107 unidentified. The identity of the CH_2 resonance signals was confirmed using a 2D DEPT NMR experiment.

The ^{19}F NMR spectrum confirmed the presence of the dissociated free aminoalcohol ligand and the hexafluoroacetone hydrate by showing two sharp signals at δ −83.12 (100) and −78.75 (99%), respectively, while the third signal at δ −77.53 (92%) is assigned to the third compound observed in the ^{1}H NMR spectrum. Based on these ^{1}H and ^{19}F NMR data and the subsequent GC-MS analysis, which shows a weak parent ion at m/z = 265 and a base peak at m/z = 250 due to the M^+ − Me ion, we can identify this unknown compound as a CF_3-substituted 1,3-oxazolidine (**7**).

If the assignment of this organic compound is correct, we can then postulate that its formation may involve a thermally-induced, bimolecular condensation between the dissociated imine $H_2C{=}NR^2$ and free aminoalcohol ligand, according to a similar reaction reported in the literature.[29]

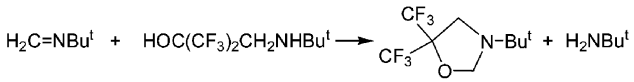

(**7**)

Moreover, the CH_2 signals at δ 4.68 and 3.29 are also observed in the ^{1}H NMR spectrum of the mixture of products obtained from a control reaction using the β-aminoalcohol reagent $HOC(CF_3)_2CH_2NHBu^t$ and iodobenzene. This reaction has been utilized to prepare both aromatic and aliphatic imines from secondary amines.[30] As a result, although we cannot rule out the first possibility, we currently favor the second reaction pathway involving the cleavage of the C(α)–C(β) bond during the deposition of copper. Of course, more detailed studies are required to fully establish and confirm this reaction mechanism.

Finally, the CVD experiments conducted at 325 °C using Ar carrier gas show that complexes **4** and **6** do not afford the anticipated copper metal, but yield only a few droplets of Cu-containing particulates on the substrate. The reduced activity for complex **6** may be the result of the lack of such a low energy pathway for copper deposition. Therefore, the aminoalkoxide chelate complexes involving the tertiary amino group are probably unsuitable as CVD source reagents. However, upon changing the carrier gas from Ar to H_2, deposition of copper metal proceeded rapidly at this temperature, and the volatile co-product collected during the CVD runs showed exclusive formation of free $HOCMe(CF_3)CH_2NMe_2$. Thus, the deposition of copper from complex **6** is best understood as shown in the equation below,

$$Cu[OCMe(CF_3)CH_2NMe_2]_2 + H_2 \rightarrow Cu_{(s)} + 2\ HOCMe(CF_3)CH_2NMe_2$$

in which the hydrogen serves as the stoichiometric reagent to reduce the copper complex during deposition.

Conclusion

Several new Cu^{II} complexes with chelating aminoalkoxide ligands have been reported in this study. Although they are all very stable at room temperature, deposition of copper metal can be achieved at a substrate temperature between 250 and 325 °C. However, as revealed by CVD experiments, the complexes with chelating alkoxide ligands bearing secondary amino groups, CH_2NHR, R = CH_2CH_2OMe, Bu^i, and Bu^t, showed a greater tendency to deposit copper metal at lower temperature, even in absence of an external reducing reagent. The deposition of copper probably proceeds *via* a self-catalyzed reduction of Cu^{II}, for which the driving force is provided by the concomitant conversion of amine to imine or the direct cleavage of the C(α)–C(β) bond. This observation is reminiscent of a recent report that addition of alcohol co-reactant in the process gas stream accelerates the reaction rate of copper deposition in an experiment using $Cu(hfac)_2$ as the source reagent.[31] It was proposed that, when N_2 is used as the carrier gas, the alcohol served as the reducing reagent. In a similar fashion, the secondary amine fragment, supplies here the hydrogen atoms that are formally required for the reduction of Cu^{II}. A preliminary CVD experiment showed that filling of a vial hole with a diameter of 0.4 μm is possible using **2** as the source reagent at a temperature of 275 °C.

Finally, the Cu^{II} fluoroalkoxide complexes **4** and **6**, containing a tertiary amino group, showed an even greater volatility and thermal stability. These physical properties were demonstrated by the TGA experiments, where rapid loss of weight was observed at a lower temperature, as well as in the actual CVD experiments, for which no deposition of copper was observed at typical deposition temperatures of 250–325 °C under an inert atmosphere. It appears that the lack of the NH functional group completely blocks the lower energy deposition pathway observed for the previous complexes possessing the secondary amine coordination group. Nevertheless, the deposition of copper metal was successfully achieved at the same temperature by changing the carrier gas from Ar to H_2, which suggests that the deposition of copper is facilitated by the hydrogenation, rather than the self-catalyzed, intramolecular disproportionation reaction involving the coordinated amine fragments.

Acknowledgements

We thank the National Science Council (NSC 90-2113-M007-022) and the Ministry of Education (89-FA-04-AA), Taiwan, and the National Research Council, Canada, for support of this work.

References

1 (*a*) W. L. Gladfelter, *Chem. Mater.*, 1993, **5**, 1372; (*b*) C. Steinbrüchel, *Appl. Surf. Sci.*, 1995, **91**, 139; (*c*) P. Doppelt, *Microelectron. Eng.*, 1997, **37/38**, 89; (*d*) V. N. Vertoprakhov and S. A. Krupoder, *Russ. Chem. Rev.*, 2000, **69**, 1057.

2 (*a*) D.-H. Kim, R. H. Wentorf and W. N. Gill, *J. Electrochem. Soc.*, 1993, **140**, 3273; (*b*) N. Awaya, K. Ohno and Y. Arita, *J. Electrochem. Soc.*, 1995, **142**, 3173; (*c*) Y. D. Chen, A. Reisman, I. Turlink and D. Temple, *J. Electrochem. Soc.*, 1995, **142**, 3903.

3 (*a*) H. Choi and S. Hwang, *Chem. Mater.*, 1998, **10**, 2326; (*b*) S. M. Fine, P. N. Dyer, J. A. T. Norman, B. A. Muratore and R. L. Lampietro, *Mater. Res. Soc. Symp. Proc.*, 1990, **204**, 415; (*c*) S. Hwang, H. Choi and I. Shim, *Chem. Mater.*, 1996, **8**, 981; (*d*) A. Devi, J. Goswami, R. Lakshmi, S. A. Shivashankar and S. Chandrasekaran, *J. Mater. Res.*, 1998, **13**, 687.

4 (*a*) C. Oehr and H. Suhr, *Appl. Phys. A.*, 1988, **45**, 151; (*b*) W. G. Lai, Y. Xie and G. L. Griffin, *J. Electrochem. Soc.*, 1991, **138**, 3499; (*c*) A. E. Kaloyeros, A. Feng, J. Garhart, K. C. Brooks, S. K. Ghosh, A. N. Saxena and F. Luehrs, *J. Electron. Mater.*, 1990, **19**, 271; (*d*) N. S. Borgharkar and G. L. Griffin, *J. Electrochem. Soc.*, 1998, **145**, 347.

5 D. Temple and A. Reisman, *J. Electrochem. Soc.*, 1989, **136**, 3525.
6 D. B. Beach, F. K. LeGoues and C. K. Hu, *Chem. Mater.*, 1990, **2**, 216.
7 (*a*) R. Kumar, F. R. Fronczek, A. W. Maverick, W. G. Lai and G. L. Griffin, *Chem. Mater.*, 1992, **4**, 577; (*b*) A. Jain, K. M. Chi, M. J. Hampden-Smith, T. T. Kodas, J. D. Farr and M. F. Paffett, *J. Mater. Res.*, 1992, **7**, 261.
8 (*a*) P. Doppelt, *Coord. Chem. Rev.*, 1998, **178–180**, 1785; (*b*) M. B. Naik, W. N. Gill, R. H. Wentorf and R. R. Reeves, *Thin Solid Films*, 1995, **262**, 60; (*c*) V. M. Donnelly and M. E. Gross, *J. Vac. Sci. Technol.*, 1993, **11**, 66; (*d*) M. J. Hampden-Smith and T. Kodas, *Polyhedron*, 1995, **14**, 699; (*e*) T.-Y. Chen, J. Vaissermann, E. Ruiz, J. P. Senateur and P. Doppelt, *Chem. Mater.*, 2001, **13**, 3993.
9 (*a*) A. Jain, K. M. Chi, T. T. Kodas and M. J. Hampden-Smith, *J. Electrochem. Soc.*, 1993, **140**, 1434; (*b*) M. L. H. ter Heerdt, P. J. van der Put and J. Schoonman, *Chem. Vap. Deposition*, 2001, **7**, 199.
10 (*a*) J. A. T. Norman, D. A. Robert, A. K. Hochberg, P. Smith, G. A. Peterson, J. E. Parmeter, C. A. Apblett and T. R. Omstead, *Thin Solid Films*, 1995, **262**, 46; (*b*) M.-Y. Park, J.-H. Son, S.-W. Kang and S.-W. Rhee, *J. Mater. Res.*, 1999, **14**, 975.
11 (*a*) M. E. Gross, *J. Electrochem. Soc.*, 1991, **138**, 2422; (*b*) M. J. Hampden-Smith and T. T. Kodas, *Chem. Vap. Deposition*, 1995, **1**, 8.
12 P.-F. Hsu, Y. Chi, T.-W. Lin, C.-S. Liu, A. J. Carty and S.-M. Peng, *Chem. Vap. Deposition*, 2001, **7**, 28.
13 (*a*) I.-S. Chang and C. J. Willis, *Can. J. Chem.*, 1977, **55**, 2465; (*b*) S. J. Loeb, J. F. Richardson and C. J. Willis, *Inorg. Chem.*, 1983, **22**, 2736.
14 G. M. Sheldrick, SHELXTL/PC, Program for Crystal Structure Determination, Siemens Analytical X-Ray Instruments, Inc., Madison, WI, USA, 1994.
15 SAINT, Program for Area Detector Absorption Correction, Siemens Analytical X-Ray Instruments, Inc., Madison, WI, USA, 1994.
16 Y. Chi, S. Ranjan, T.-Y. Chou, C.-S. Liu, S.-M. Peng and G.-H. Lee, *J. Chem. Soc., Dalton Trans.*, 2001, 2462.
17 P. M. Jeffries, S. R. Wilson and G. S. Girolami, *Inorg. Chem.*, 1992, **31**, 4503.
18 J. Pinkas, J. C. Huffman, J. C. Bollinger, W. E. Streib, D. V. Baxter, M. H. Chisholm and K. G. Caulton, *Inorg. Chem.*, 1997, **36**, 2930.
19 Y.-B. Dong, M. D. Smith, R. C. Layland and H.-C. zur Loye, *Inorg. Chem.*, 1999, **38**, 5027.
20 A. Jain, T. T. Kodas, T. S. Corbitt and M. J. Hampden-Smith, *Chem. Mater.*, 1996, **8**, 1119.
21 C.-H. Chang, K. C. Hwang, C.-S. Liu, Y. Chi, A. J. Carty, L. Scoles, S.-M. Peng, G.-H. Lee and J. Reedijk, *Angew. Chem., Int. Ed.*, 2001, **40**, 4651.
22 A. C. Jones, *Chem. Vap. Deposition*, 1998, **4**, 169.
23 S. M. Sze, *VLSI Technology*, McGraw-Hill, New York, 2nd edn., 1988, p. 411.
24 S. C. Goel, K. S. Kramer, M. Y. Chiang and W. E. Buhro, *Polyhedron*, 1990, **9**, 611.
25 Y. K. Chae and H. Komiyama, *J. Appl. Phys.*, 2001, **90**, 3610.
26 (*a*) S. C. Goel and W. E. Buhro, *Inorg. Synth.*, 1997, **31**, 294; (*b*) V. L. Young, D. F. Cox and M. E. Davis, *Chem. Mater.*, 1993, **5**, 1701.
27 J. Yamaguchi and T. Takeda, *Chem. Lett.*, 1992, 1933.
28 (*a*) L. C. Portis, J. T. Kulg and K. Mann, *J. Org. Chem.*, 1974, **39**, 3488; (*b*) M. Masui, Y. Kamada, E. Sasaki and S. Ozaki, *Chem. Pharm. Bull.*, 1982, **30**, 1234.
29 (*a*) T. Nishiyama, H. Kishi, K. Kitano and F. Yamada, *Bull. Chem. Soc. Jpn.*, 1994, **67**, 1765; (*b*) K. Ito and S. Miyajima, *J. Heterocycl. Chem.*, 1997, **34**, 501.
30 J. Larsen and K. A. Jorgensen, *J. Chem. Soc., Perkin Trans.*, 1992, **2**, 1213.
31 N. S. Borgharkar, G. L. Griffin, A. James and A. W. Maverick, *Thin Solid Films*, 1998, **320**, 86.